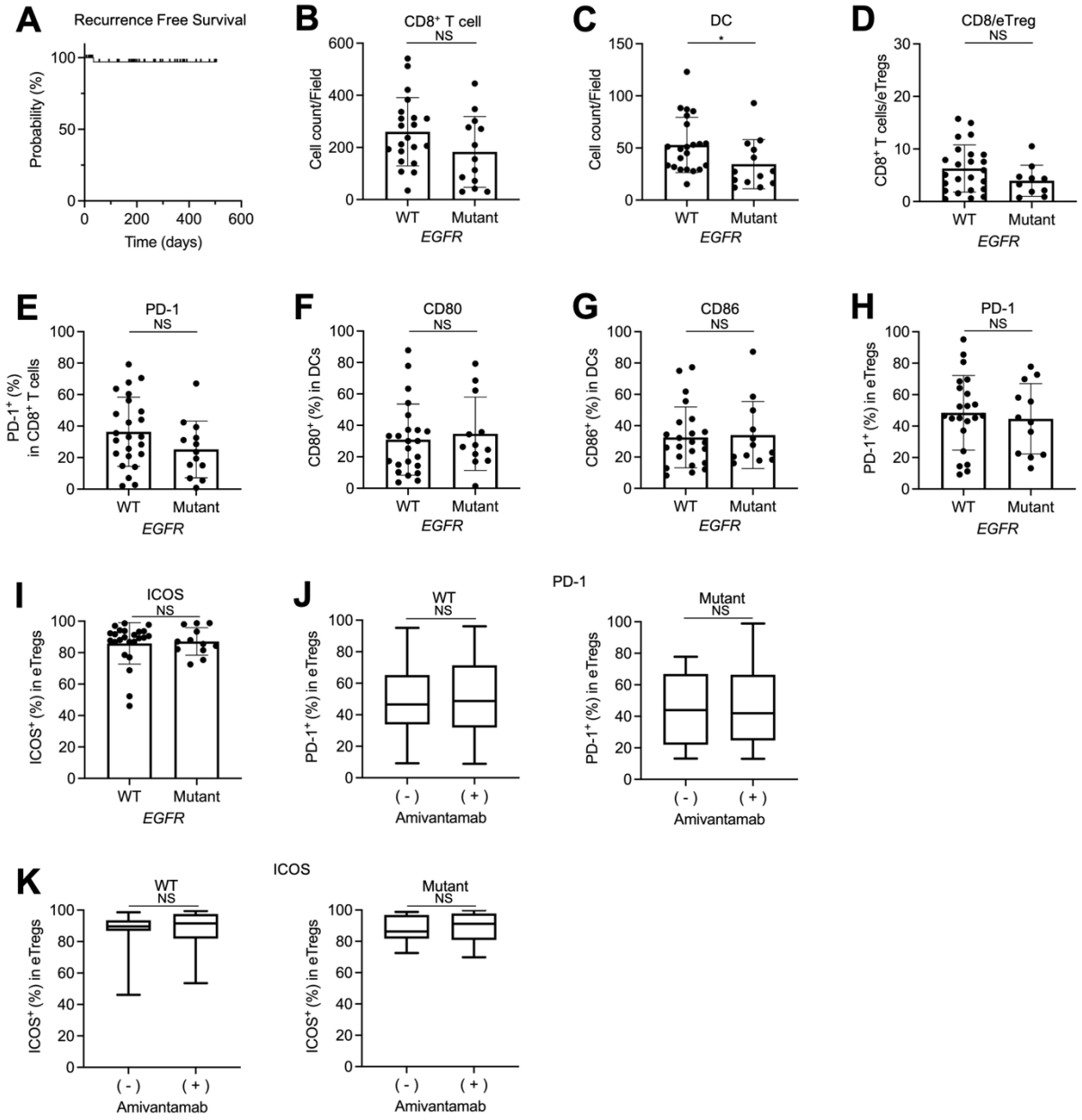

Figure S1. Baseline immune profiles and additional amivantamab-induced changes according to *epidermal growth factor receptor* (*EGFR*) mutation status.

(A) Recurrence-free survival. Recurrence-free survival was defined as the time from the date of surgery to the date of the first documented recurrence or death from any cause, and the Kaplan–Meier curve is shown.

(B, C) Immunohistochemistry (IHC) analyses of tumor samples stratified by *EGFR* mutation status. Summaries of $CD8^+$ T cell (B) and $CD11c^+$ dendritic cell (DC) (C) infiltration according to *EGFR* mutation status are shown.

(D–I) Flow cytometric analyses of tumor-infiltrating lymphocytes (TILs) stratified by *EGFR* mutation status. Freshly resected non-small cell lung cancer (NSCLC) tumor digests were directly analyzed by flow cytometry without any treatment. Summaries of tumor-infiltrating $CD8^+$ T cell/effector regulatory T cell (eTreg) ratio (D), programmed cell death-1 (PD-1) expression in

tumor-infiltrating $CD8^+$ T cells (E), CD80 (F) and CD86 (G) expression in tumor-infiltrating DCs, and PD-1 (H) and inducible T-cell co-stimulator (ICOS) (I) expression in tumor-infiltrating eTregs according to *EGFR* mutation status are shown.
(J, K) Amivantamab-induced changes in tumor-infiltrating eTregs stratified by *EGFR* mutation status. The e*x vivo* TIL assays were performed as described in **Figure 1A**. PD-1 (J) and ICOS (K) expression according to *EGFR* mutation status are shown.

Statistical analyses were performed by t-tests in (B-K). Each dot represents an individual sample and data are represented as the mean ± SD in (B-I). In box-and-whisker plots, the box spans from the first to the third quartile with a line at the median and the whiskers extend from the minimum to the maximum in (J) and (K). NS: not significant; $^*P < 0.05$.

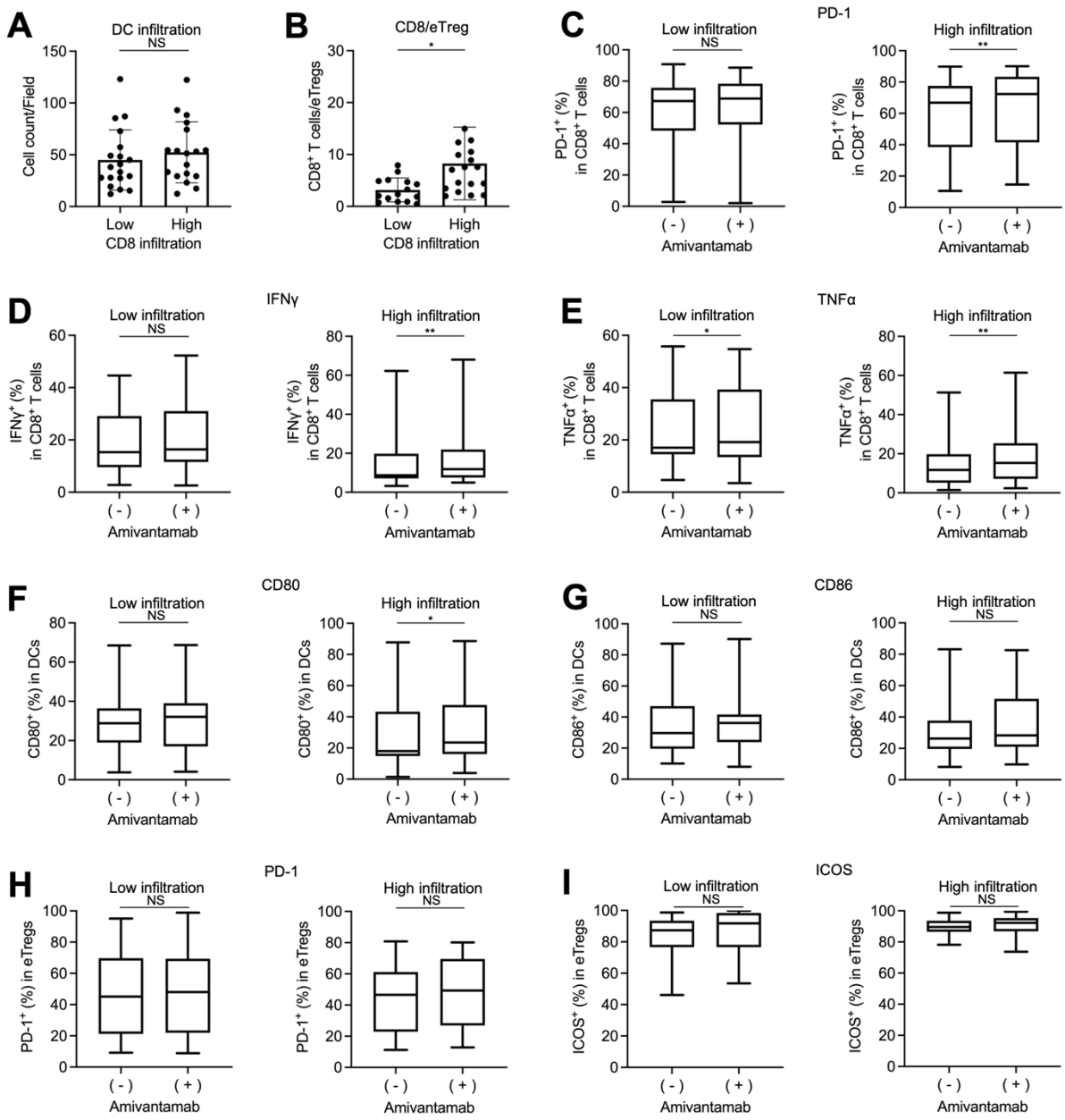

Figure S2. Baseline immune profiles and additional amivantamab-induced changes according to CD8⁺ T-cell infiltration.

(A) CD11c⁺ dendritic cell (DC) infiltration stratified by CD8⁺ T-cell infiltration. CD8⁺ T cell and CD11c⁺ DC infiltration were analyzed by immunohistochemistry (IHC) and the median value was used as the cut-off for CD8⁺ T-cell infiltration.

(B) CD8⁺ T cell/effector regulatory T cell (eTreg) ratio of tumor-infiltrating lymphocytes (TILs) stratified by CD8⁺ T-cell infiltration. Freshly resected non-small cell lung cancer (NSCLC) tumor digests were directly analyzed by flow cytometry without any treatment.

(C–I) Amivantamab-induced changes in TILs stratified by CD8⁺ T-cell infiltration. The *ex vivo* TIL assays were performed as described in **Figure 1A**. Summaries of programmed cell death-1 (PD-1) expression (C), interferon-γ (IFNγ) production (D), and tumor necrosis factor-α (TNFα) production (E) in tumor-infiltrating CD8⁺ T cells, CD80 (F) and CD86 (G) expression in tumor-

infiltrating DCs, and PD-1 (H) and inducible T-cell co-stimulator (ICOS) (I) expression in tumor-infiltrating eTregs according to $CD8^+$ T-cell infiltration are shown.

Statistical analyses were performed by t-tests. Each dot represents an individual sample and data are represented as the mean ± SD in (A) and (B). In box-and-whisker plots, the box spans from the first to the third quartile with a line at the median and the whiskers extend from the minimum to the maximum in (C-I). NS: not significant; $^{*}P < 0.05$, $^{**}P < 0.01$.

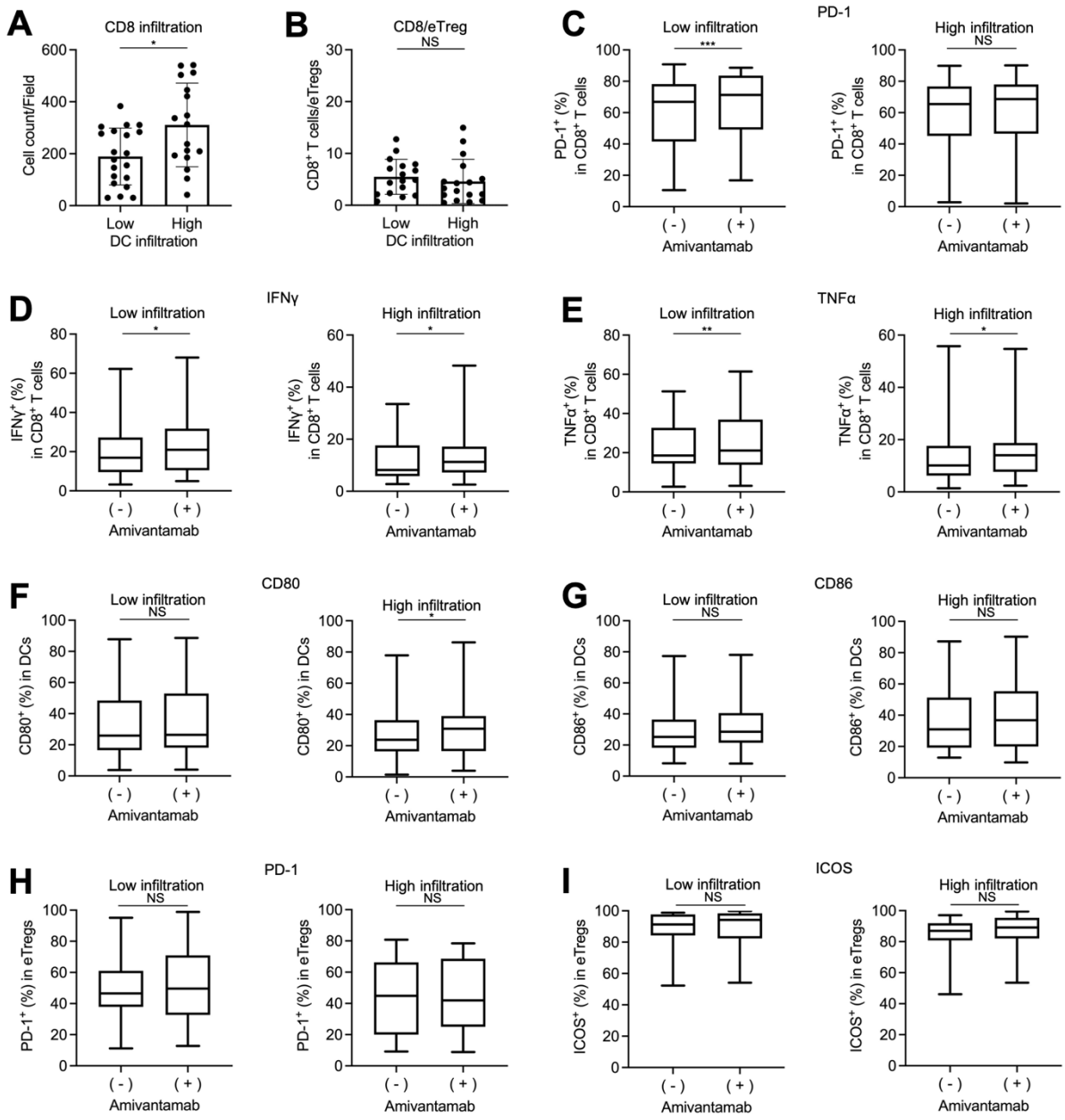

Figure S3. Baseline immune profiles and additional amivantamab-induced changes according to CD11c$^+$ dendritic cell (DC) infiltration.

(A) CD8$^+$ T-cell infiltration stratified by CD11c$^+$ DC infiltration. CD8$^+$ T cell and CD11c$^+$ DC infiltration were analyzed by immunohistochemistry (IHC) and the median value was used as the cut-off for CD11c$^+$ DC infiltration.

(B) CD8$^+$ T cell/ effector regulatory T cell (eTreg) ratio of tumor-infiltrating lymphocytes (TILs) stratified by CD11c$^+$ DC infiltration. Freshly resected non-small cell lung cancer (NSCLC) tumor digests were directly analyzed by flow cytometry without any treatment.

(C–I) Amivantamab-induced changes in TILs stratified by CD11c$^+$ DC infiltration. The *ex vivo* TIL assays were performed as described in **Figure 1A**. Summaries of programmed cell death-1 (PD-1) expression (C), interferon-γ (IFNγ) production (D), and tumor necrosis factor-α (TNFα) production (E) in tumor-infiltrating CD8$^+$ T cells, CD80 (F) and CD86 (G) expression in tumor-

infiltrating DCs, and PD-1 (H) and inducible T-cell co-stimulator (ICOS) (I) expression in tumor-infiltrating eTregs according to $CD11c^+$ DC infiltration are shown.

Statistical analyses were performed by t-tests. Each dot represents an individual sample and data are represented as the mean ± SD in (A) and (B). In box-and-whisker plots, the box spans from the first to the third quartile with a line at the median and the whiskers extend from the minimum to the maximum in (C-I). NS: not significant; $^{*}P < 0.05$, $^{**}P < 0.01$; $^{***}P < 0.001$.

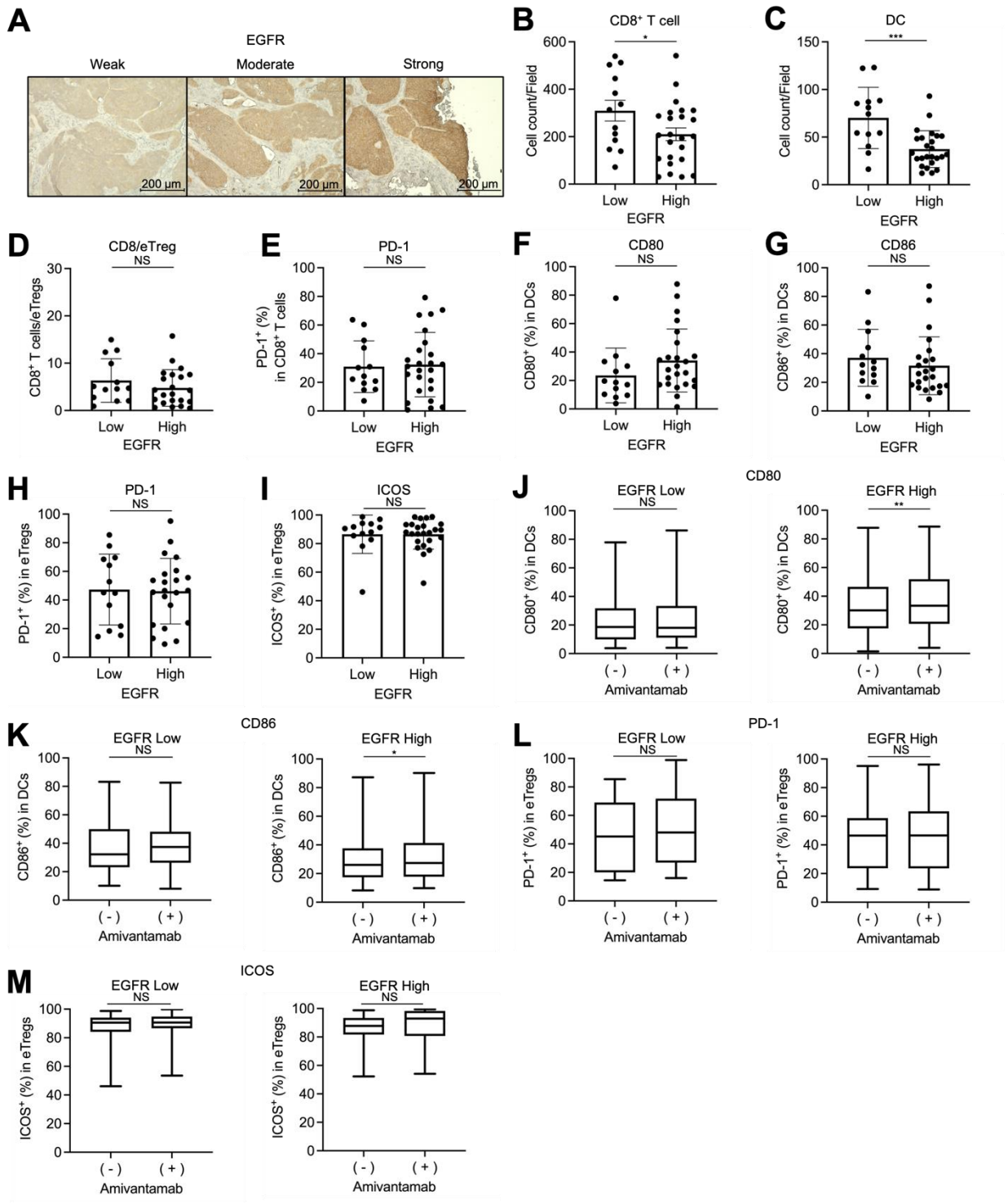

Figure S4. Baseline immune profiles and additional amivantamab-induced changes according to epidermal growth factor receptor (EGFR) expression level.

(A) Representative immunohistochemistry (IHC) staining for EGFR.

(B, C) $CD8^+$ T-cell (B) and $CD11c^+$ dendritic cell (DC) (C) infiltration stratified by EGFR expression level. The EGFR expression levels were defined as described in **Figure 3**. $CD8^+$ T cell and $CD11c^+$ DC infiltration were analyzed by IHC.

(D–I) Flow cytometric analyses of tumor-infiltrating lymphocytes (TILs) stratified by EGFR expression level. Freshly resected non-small cell lung cancer (NSCLC) tumor digests were directly analyzed by flow cytometry without any treatment. Summaries of tumor-infiltrating $CD8^+$ T cell/effector regulatory T cell (eTreg) ratio (D), programmed cell death-1 (PD-1) expression in tumor-infiltrating $CD8^+$ T cells (E), CD80 (F) and CD86 (G) expression in tumor-infiltrating DCs, and PD-1 (H) and inducible T-cell co-stimulator (ICOS) (I) expression in tumor-infiltrating eTregs according to EGFR expression level are shown.
(J–M) Amivantamab-induced changes in TILs stratified by EGFR expression level. The *ex vivo* TIL assays were performed as described in **Figure 1A**. Summaries of CD80 (J) and CD86 (K) expression in tumor-infiltrating DCs, and PD-1 (L) and ICOS (M) expression in tumor-infiltrating eTregs according to EGFR expression level are shown.

Statistical analyses were performed by t-tests in (B-M). Each dot represents an individual sample and data are represented as the mean ± SD in (B-I). In box-and-whisker plots, the box spans from the first to the third quartile with a line at the median and the whiskers extend from the minimum to the maximum in (J-M). NS: not significant; $^{*}P < 0.05$, $^{**}P < 0.01$; $^{***}P < 0.001$.

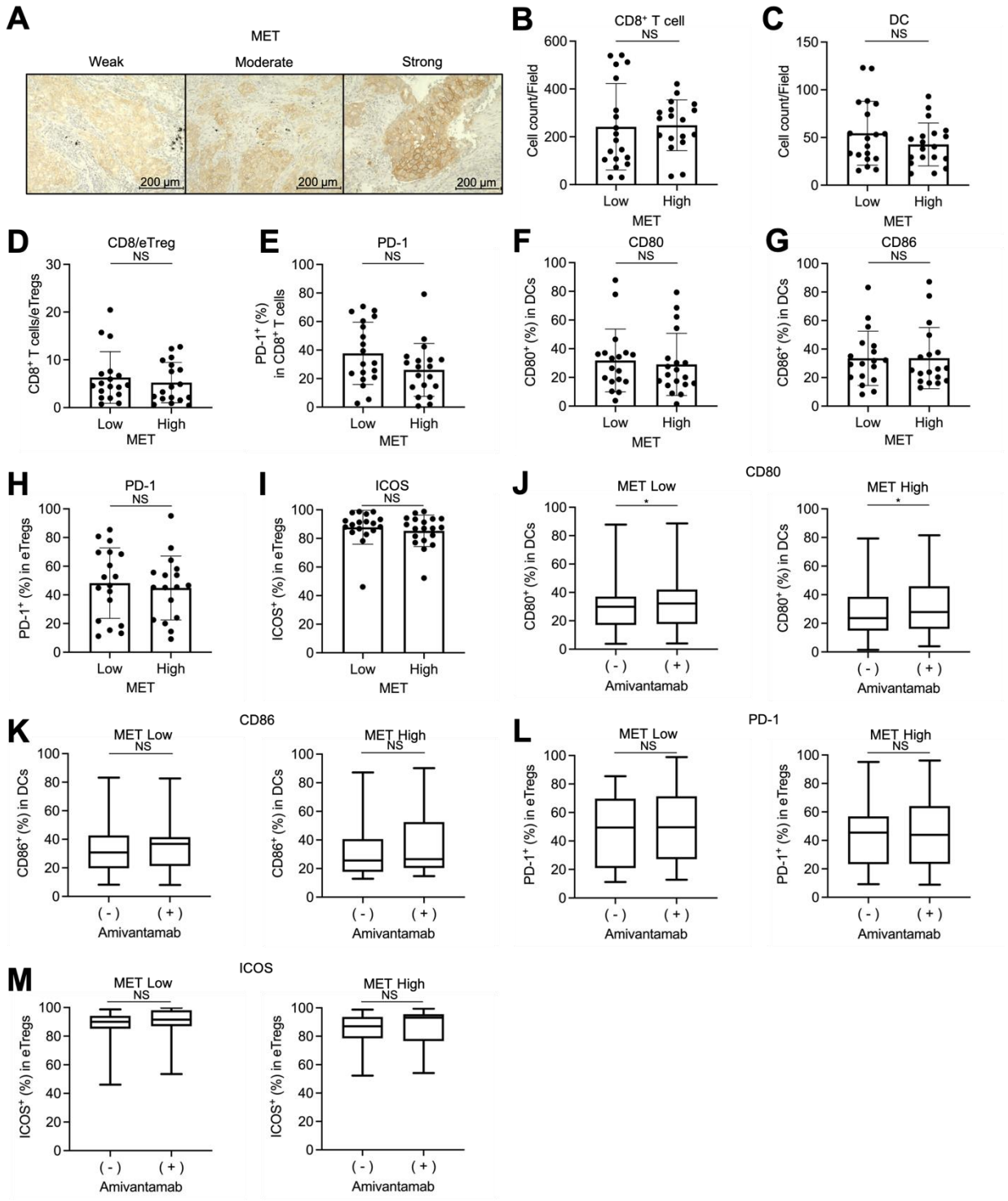

Figure S5. Baseline immune profiles and additional amivantamab-induced changes according to MNNG HOS Transforming (MET) expression level.

(A) Representative immunohistochemistry (IHC) staining for MET.

(B, C) $CD8^+$ T-cell (B) and $CD11c^+$ dendritic cell (DC) (C) infiltration stratified by MET expression level. The MET expression levels were defined as described in **Figure 3.** $CD8^+$ T cell and $CD11c^+$ DC infiltration were analyzed by IHC.

(D–I) Flow cytometric analyses of tumor-infiltrating lymphocytes (TILs) stratified by MET expression level. Freshly resected non-small cell lung cancer (NSCLC) tumor digests were directly analyzed by flow cytometry without any treatment. Summaries of tumor-infiltrating $CD8^+$ T cell/effector regulatory T cell (eTreg) ratio (D), programmed cell death-1 (PD-1) expression in tumor-infiltrating $CD8^+$ T cells (E), CD80 (F) and CD86 (G) expression in tumor-infiltrating DCs, and PD-1 (H) and inducible T-cell co-stimulator (ICOS) (I) expression in tumor-infiltrating eTregs according to MET expression level are shown.
(J–M) Amivantamab-induced changes in TILs stratified by MET expression level. The *ex vivo* TIL assays were performed as described in **Figure 1A**. Summaries of CD80 (J) and CD86 (K) expression in tumor-infiltrating DCs, and PD-1 (L) and ICOS (M) expression in tumor-infiltrating eTregs according to MET expression level are shown.

Statistical analyses were performed by t-tests in (B-M). Each dot represents an individual sample and data are represented as the mean ± SD in (B-I). In box-and-whisker plots, the box spans from the first to the third quartile with a line at the median and the whiskers extend from the minimum to the maximum in (J-M). NS: not significant; $^*P < 0.05$.

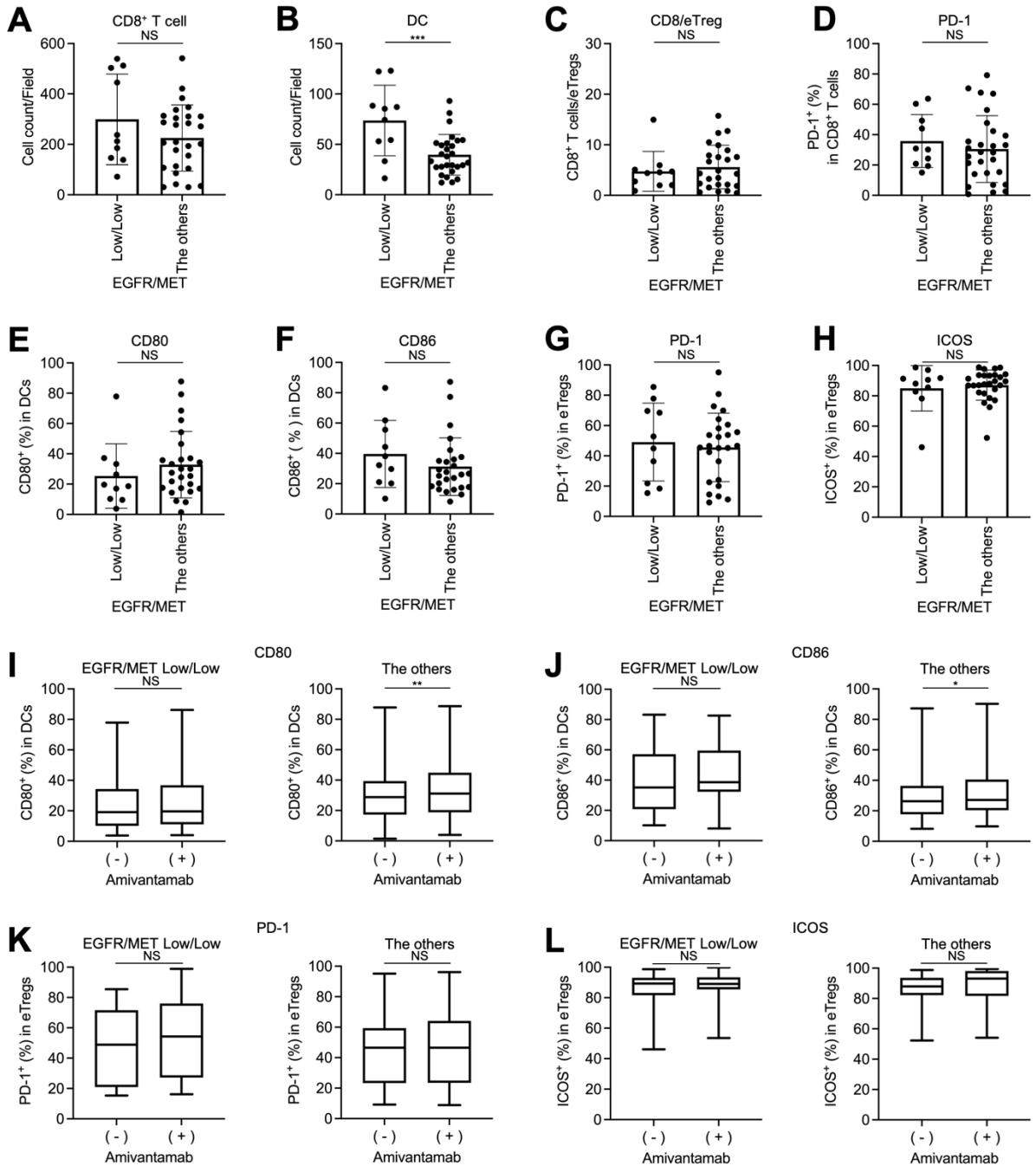

Figure S6. Baseline immune profiles and additional amivantamab-induced changes according to epidermal growth factor receptor (EGFR)/MNNG HOS Transforming (MET) expression level.

(A, B) $CD8^+$ T-cell (A) and $CD11c^+$ dendritic cell (DC) (B) infiltration stratified by EGFR/MET expression level. The EGFR/MET expression levels were defined as described in **Figure 3.** $CD8^+$ T cell and $CD11c^+$ DC infiltration were analyzed by IHC.

(C–H) Flow cytometric analyses of tumor-infiltrating lymphocytes (TILs) stratified by EGFR/MET expression level. Freshly resected non-small cell lung cancer (NSCLC) tumor digests were directly analyzed by flow cytometry without any treatment. Summaries of tumor-infiltrating

$CD8^+$ T cell/effector regulatory T cell (eTreg) ratio (C), programmed cell death-1 (PD-1) expression in tumor-infiltrating $CD8^+$ T cells (D), CD80 (E) and CD86 (F) expression in tumor-infiltrating DCs, and PD-1 (G) and inducible T-cell co-stimulator (ICOS) (H) expression in tumor-infiltrating eTregs according to EGFR/MET expression level are shown.
(I–L) Amivantamab-induced changes in TILs stratified by EGFR/MET expression level. The *ex vivo* TIL assays were performed as described in **Figure 1A**. Summaries of CD80 (I) and CD86 (J) expression in tumor-infiltrating DCs, and PD-1 (K) and ICOS (L) expression in tumor-infiltrating eTregs according to EGFR/MET expression level are shown.

Statistical analyses were performed by t-tests. Each dot represents an individual sample and data are represented as the mean ± SD in (A-H). In box-and-whisker plots, the box spans from the first to the third quartile with a line at the median and the whiskers extend from the minimum to the maximum in (I-L). NS: not significant; $^{*}P < 0.05$, $^{**}P < 0.01$; $^{***}P < 0.001$.

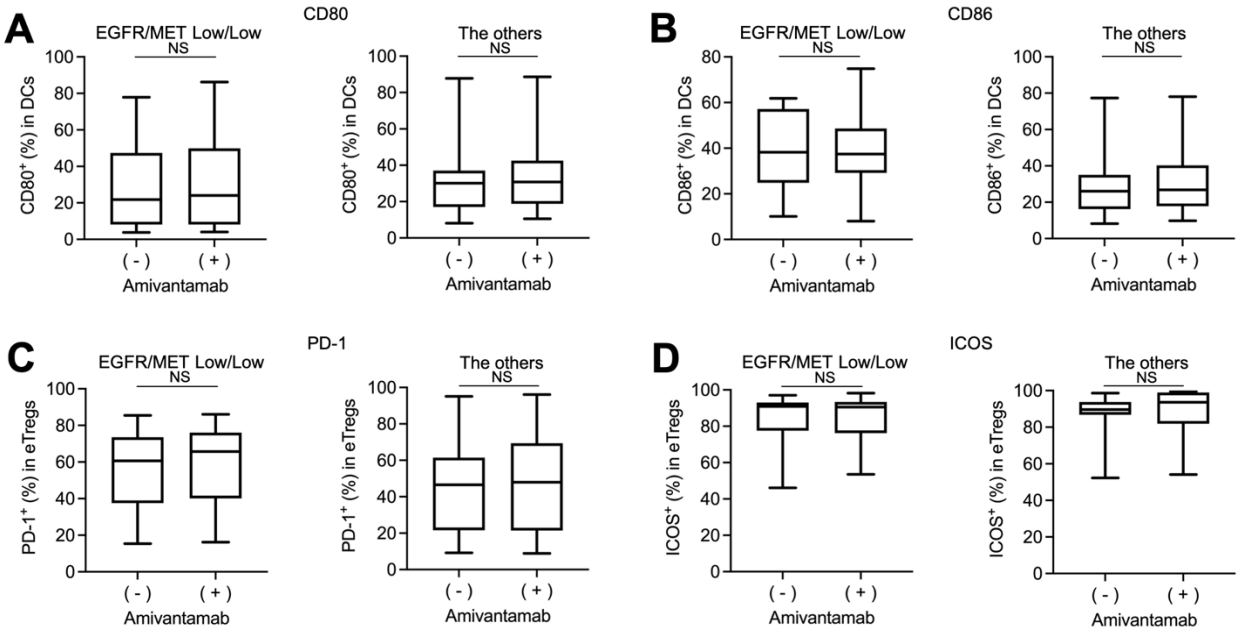

Figure S7. Additional amivantamab-induced changes according to epidermal growth factor receptor (EGFR)/MNNG HOS Transforming (MET) expression level in *EGFR*-wild type (WT) tumors.

(A–D) Amivantamab-induced changes in tumor-infiltrating lymphocytes (TILs) stratified by EGFR/MET expression level in EGFR-WT tumors. The *ex vivo* TIL assays were performed as described in **Figure 1A**. The EGFR/MET expression levels were defined as described in **Figure 3.** Summaries of CD80 (A) and CD86 (B) expression in tumor-infiltrating dendritic cells (DCs), and programmed cell death-1 (PD-1) (C) and inducible T-cell co-stimulator (ICOS) (D) expression in tumor-infiltrating effector regulatory T cells (eTregs) according to EGFR/MET expression level in *EGFR*-WT tumors are shown.

Statistical analyses were performed by t-tests. In box-and-whisker plots, the box spans from the first to the third quartile with a line at the median and the whiskers extend from the minimum to the maximum. NS: not significant.

Table S1. Patient characteristics (n = 40)

Patient characteristics	Number (%)
Sex, male	29 (73)
Age, ≥75	21 (53)
Smoking history, yes	27 (68)
Histological subtypes	
Adenocarcinoma	32 (80)
The others	8 (20)
Postoperative pathological staging	
I	23 (58)
II	12 (30)
III	4 (10)
EGFR mutation, yes	13/37 (35)
MET exon 14 skipping mutation, yes	2/16 (13)
Smoking history, yes	27 (68)
Performance status	
0	38 (95)
1	2 (5)
Neoadjuvant chemotherapy	
Combination immunotherapy	2 (5)
Postoperative recurrence (< 6 months), yes	1 (3)
Postoperative deaths (< 6 months), yes	0 (0)

Abbreviations: *EGFR*, *epidermal growth factor receptor*; *MET, MNNG HOS Transforming.*

Table S2. Anti-human antibodies used for multicolor flow cytometry

Molecule	Clone	Company	Conjugation	RRID
CD3	UCHT1	Biolegend	Alexa Fluor 700	AB_493741
CD4	SK3	BD Biosciences	BV510	AB_2744424
CD8a	RPA-T8	Biolegend	FITC	AB_2562055
CD11c	3.9	Biolegend	BV711	AB_ 2562192
CD14	M5E2	Biolegend	Alexa Fluor 700	AB_493747
CD19	SJ25C1	Biolegend	Alexa Fluor 700	AB_2616935
CD45RA	HI100	BD Biosciences	PerCP-Cy5.5	AB_2738199
CD56 (NCAM)	HCD56	Biolegend	Alexa Fluor 700	AB_604104
CD80	2D10	Biolegend	PE-Cy7	AB_2076148
CD86	IT2.2	Biolegend	PE-Cy5	AB_314528
CD278 (ICOS)	C398.4A	Biolegend	BV605	AB_2687079
CD279 (PD-1)	MIH4	BD Biosciences	BV421	AB_2738745
FOXP3	259D/C7	BD Biosciences	PE	AB_1645508
HLA-DR	G46-6	BD Biosciences	APC	AB_398674
IFNγ	B27	BD Biosciences	BV605	AB_2737926
TNFα	MAb11	Biolegend	BV711	AB_2563885

Abbreviations: NCAM, neural cell adhesion molecule; ICOS, inducible T-cell co-stimulator; PD-1, programmed cell death-1; IFNγ, interferon-γ; TNFα, tumor necrosis factor-α.